



# Analysis of Cell to Module Loss Factor for Shingled PV Module

Sanchari Chowdhury<sup>1)</sup> · Eun–Chel Cho<sup>2)</sup> · Younghyun Cho<sup>2)</sup> · Youngkuk Kim<sup>2)\*</sup> · Junsin Yi<sup>3)\*</sup>

Received 10 April 2020 Revised 28 August 2020 Accepted 1 September 2020 Published online 21 September 2020

**ABSTRACT** Shingled technology is the latest cell interconnection technology developed in the photovoltaic (PV) industry due to its reduced resistance loss, low-cost, and innovative electrically conductive adhesive (ECA). There are several advantages associated with shingled technology to develop cell to module (CTM) such as the module area enlargement, low processing temperature, and interconnection; these advantages further improves the energy yield capacity. This review paper provides valuable insight into CTM loss when cells are interconnected by shingled technology to form modules. The fill factor (FF) had improved, further reducing electrical power loss compared to the conventional module interconnection technology. The commercial PV module technology was mainly focused on different performance parameters; the module maximum power point (P<sub>mpp</sub>), and module efficiency. The module was then subjected to anti-reflection (AR) coating and encapsulant material to absorb infrared (IR) and ultraviolet (UV) light, which can increase the overall efficiency of the shingled module by up to 24.4%. Module fabrication by shingled interconnection technology uses EGAIn paste; this enables further increases in output power under standard test conditions. Previous research has demonstrated that a total module output power of approximately 400 Wp may be achieved using shingled technology and CTM loss may be reduced to 0.03%, alongside the low cost of fabrication.

**Key words** Shingled module, CTM analysis, Cell interconnection, Cell spacing, Encapsulant

## Nomenclature

$\lambda$	: wavelength, nm
R	: reflection coefficient
P <sub>mpp</sub>	: maximum power point
$\eta_{\text{cell}}$	: cell efficiency
$\eta_{\text{module}}$	: module efficiency
$\alpha$	: absorption coefficient

## Subscript

CTM	: cell-to-module
PV	: photovoltaic
AR	: anti-reflection
UV	: ultra-violet
PERC	: passivated emitter and rear cell
FZ	: float zone
Cz Si	: czochralski silicon
EGAIn	: eutectic gallium and indium
POE	: polyolefin
PVB	: polyvinyl butyral
TPT	: tedlar / polyester / tedlar

1) Ph.D. Candidate, College of Information and Communication Engineering, Sungkyunkwan University

2) Research Professor, College of Information and Communication Engineering, Sungkyunkwan University

3) Professor, College of Information and Communication Engineering, Sungkyunkwan University

\*Corresponding authors: junsin@skku.edu (JSY);  
bri3tain@skku.edu (YGK)

Tel: +82-31-290-7139

## 1. Introduction

Shingled technology was commercially available from 2005<sup>[1]</sup>. Research studies at that time estimated that this technology can generate up to \$10 billion by the end of 2020<sup>[2]</sup>. Many commercial industries in solar cell adapted shingled technology due to its simple fabrication process and lower cost. The shingling technology allowed to further boost output power of the module by using an advanced technology for cell interconnection by employing overlapping adjacent cells. A combination of optimized reflective surface and their slant height during installations can achieve an additional energy generation of up to 25%. Shingled module can increase the output power up to 10.3% and efficiency of 15% compared to conventional modules. In this new field of technology, it is possible to further reduce the cost of energy generated by photovoltaic modules for the required applications. The shingled solar cells are also found to be like the p-type PERC solar cells. The advantage of shingled module technology is it can be used in solar roof tiles. As the global demand of solar technology are increasing strongly, PV industries mainly focus the increase in module efficiency with higher output power. Terrestrial applications of shingled technology are considered aiming at increased module power and efficiency without changing the module area. In several research institute, shingling technology has become an interesting research topic for module manufacturing worldwide<sup>[3-5]</sup>. Shingled technology mainly focuses on the number of cell strips and the cell front to rear interconnection technique. Here, the cell stripes are connected in a single manner, similar to roof tiles. One of the easiest ways to reduce resistance loss is by replacing the number of bus bars with HIP MWT technique. The current market trend shows the mono-facial cell-based modules fabricated by shingling technology having good impact

in the PV market and there is continuous increase of interest in this field and patents<sup>[6-9]</sup>. The main aim of using this technology is to increase  $P_{mpp}$  and module efficiency with minimum CTM power loss.

## 2. About shingled PV module

### 2.1 Performances and Challenges

PV module manufacturing industries is becoming the primary resource of clean energy. This report provides emphasis on the technological developments in field of commercialized PV solar modules. A shingled module can generate more energy compared to other modules due to improved methodology with the same power rating under the standard test conditions. The generated energy mainly depends on factors (i) installation of the solar module and (ii) the light reflectance of the surface. Implementing glass in a module protects it from environmental as well as gives mechanical strength to a module. The manufactures use the glass-glass module at an industrial scale, the new shingled product also profits, in the same way forming a mature technological process. The shingling technology allowed to further boost  $P_{out}$  by employing the overlapping of adjacent cells. HIP MWT superimposed on its neighbored cells active area using an interconnection technique. With this new field of technology, it is possible to further reduce the cost of energy generated by photovoltaic modules for all applications.

### 2.2 Losses in Shingled cell to module

Researchers are targeting to reduce the loss factors during Module fabrication to enhance output power as well as efficiency. Accurate measurement using a simulation tool (sun simulator) for PV Solar cell to module is important to understand the loss mechanisms

and improve efficiencies<sup>[10,11]</sup>. Due to the shingling technology, applied to the solar cells and modules, there are additional CTM gains added to the module. This CTM loss mainly focus on the optical and resistive losses arising from cell spacing and interconnection<sup>[12,13]</sup>. Using  $EQE_{cell}^r$ , the light absorbed in the cells for different module structure, at standard testing condition the change in current concerning double glass structure can be calculated as shown in eq. (1)<sup>[14]</sup>.

$$\frac{\int EQE_{cell}^r(\lambda) [A_{cell}^{double-glass}(\lambda) - A_{cell}^{reference}(\lambda)] \phi_{ph,AM1.5}(\lambda) d\lambda}{\int EQE_{cell}^r(\lambda) \phi_{ph}(\lambda) d\lambda} \quad (1)$$

Where  $EQE_{cell}^f(\lambda)$  is the external quantum efficiency of the mono-facial cells used to develop module. In mono facial cells, generally current flows concerning the potential gradient. For example, in the mono-facial cells with “H” pattern, the current flows almost to the nearest finger, then to the nearest bus bar and then along the corresponding ribbon. The CTM resistive losses can be reduced by using some advanced HIP MWT technique with strong increase in reverse current at the front contact.

### 2.3 Approaches for Loss Reduction

There are several technologies at the module level which play a vital role in improving the cell to module (CTM) power ratio. Making use of innovative technologies like cell interconnection methods, the number of strips and spacing between cells plays an important role to increase the module power ratings. This technique started recently with an increase in the number of bus bars reaching multi bus bar level (HIP MWT) while researchers already started doing without ribbon by mass-producing shingle type of cells<sup>[15]</sup>. The module manufacturers need to take care of the longevity of the module which gradually increases the production

cost. The technology thus requires innovations to reduce the cost without compromising in module quality. Recent developments saw the encapsulation and back sheet field choosing double glass on both sides for packaging the module. The module processing steps like interconnection, stringing and laminations play an important role in reducing the optical losses. Optical losses mainly occur due to reflection at various interfaces of the module layers “air-glass – encapsulant – cell”. The absorption of light from the front cover glass and EVA adds up to this. Light scattering from the cell gap in the module and the metal contacts covered with ribbons also contribute to the plus side. The new technologies are assumed to reach a CTM power gain of 100% despite the various loss mechanism in today’s PV modules<sup>[16]</sup>.

### 2.4 Shingled Cell design

Shingled cell is designed based on overlapping the front side of the busbar of a cell to the rear side bus bar of the neighboring cell leading to a metallization of bus bar less front and rear side shingled module. Complete shingled cell with overlap covering the entire bus bar not only minimizes the cell area but also the designated area which is defined as the difference between the total cell area and the overlap cell area responsible for increasing the output power by reducing inactive cell area<sup>[17]</sup>. Overlapping of the cell provides mechanical and electrical junction to adjacent cells which further minimizes the series resistance on the interconnection level. The power loss and equivalent resistance of the shingled module is given by eq. (2) and eq. (3)

$$P_{loss,pcs} = R_{eq} \left[ \frac{I_{MPPpcs}}{l_{pcs} w_{pcs}} \left( l_f + \frac{O_{pcs}}{2} \right) \frac{S_f}{2} \right]^2 n_f + R_w I_{MPPpcs}^2 \quad (2)$$

$$R_{eq} = \frac{R_e + R_{e,c} + R_f}{2} \quad (3)$$

$$R_e = \frac{1}{6} r_{sheet} \left( \frac{s_f - w_f}{l_f} \right) \quad (4)$$

$$R_{e,c} = \frac{\sqrt{r_{sheet} \rho_c}}{l_f} \text{Coth} \left( w_f \sqrt{\left( \frac{r_{sheet}}{\rho_c} \right)} \right) \quad (5)$$

$$R_f = \frac{2}{3} \rho_f \frac{l_f}{A_f} \quad (6)$$

Where  $R_e$ ,  $R_{ec}$ ,  $R_f$  are emitter resistance, emitter contact resistance, finger resistance as given in eq. (4–6) respectively. The  $w_{pcs}$  and  $l_{pcs}$  are respectively the width and length of the solar cell stripes,  $O_{pcs}$  is the overlapping between cells defined as the busbar width at the edge. P-type silicon shingled solar cells are designed based on Czochralski-grown silicon (CZ-Si) passivated emitter and rear contact cell (PERC) technology. Different overlap scenarios using PERC cell is taken into consideration for shingled module integration. It is crucial to examine the MWT area to determine the distance needed to maximize the interconnection area and short-circuit current simultaneously.

## 2.5 Losses in Cell cut process and shingled interconnection

The design of shingled module technology can increase the efficiency and power up to 33 W<sub>p</sub> and 1.86%<sub>abs</sub> as compared to ribbon-based interconnection. CTM ratio for efficiency and power is improved mainly with ribbon or wire cell interconnection<sup>[18]</sup>. In the commercial process of Shingled technology manufacturing, the power losses can be measured as given in eq. (7).

$$P_{loss} = \Delta P_{cell\ binning} + \Delta P_{separation} + \Delta P_{manufacturing} \quad (7)$$

The shingled module is having higher impact in recent days due to the loss factors are of nearly zero value. Initially, commercial cell efficiency was

21.6% and the CTM ratio for power efficiency was 93.5%. Similarly, the output power of the module reached approximately 335.8 Wp and the CTM power ratio of 99.4%<sup>[19–21]</sup>. Shingled cells are interconnected using different materials like electrically conductive adhesive (ECA). Basically, ECA depends on time–pressure, auger or jetting. The adhesive can resist more stress absorbing than solder and hence can withstand rigors of thermal cycling and process at low temperatures. Cost of ECA is half of pure silver filled conductive adhesives. Additional feature is that the conductive adhesives is designed to cure in seconds at 150°C to 180°C to enable fast filled conductive adhesives. ECA's are used to electrically interconnect solar cells using ribbons or direct cell to cell contact. The p–n junction material bulk resistivity  $\rho_{bulk}$  and contact resistivity  $\rho_{contact}$  needs to be taken into consideration. From the Fig. 1, the electrical resistance  $R$  of an ECA–interconnection can be expressed as given in eq. (8)

$$R = \frac{\rho_{Bulk} \times thickness_{ECA}}{A_{metallization}} + 2 * \frac{\rho_{contact}}{A_{metallization}} \quad (8)$$

A shingled module is developed with the important features with 66 shingled cell per module having string distance of 2 mm using 6 strings. The following features are (i) low-iron glass with anti-reflective coating, (ii) 3.2 mm thickness, (iii) Encapsulant foil thickness of 0.45 mm with a low UV cut-off (iv) white TPT. It is assumed for a shingled module, the thickness of interconnection material (ECA) is appro–

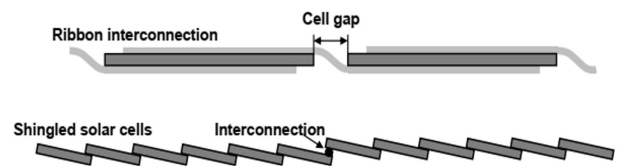


Fig. 1. Introduction of a shingled solar cell using ribbon

approximately 50  $\mu\text{m}$  having specific resistance of 0.1  $\mu\Omega/\text{m}$ . Size of a monocrystalline shingled cell is 156.75  $\times$  26  $\text{mm}^2$  and efficiency of 23.6% (0.88 $W_p$ ). Module dimensions are 1,667  $\times$  998  $\text{mm}$  (1.66  $\text{m}^2$ ) with margins of 33  $\text{mm}$  (top, bottom) and 23.75  $\text{mm}$  (left, right) assuming a cell overlap of 1  $\text{mm}$ .

$$\eta_{\text{efficiency}} = \frac{P_{\text{module}}}{E_{\text{STC}} \cdot (A_{\text{margin}} + A_{\text{cell spacing}} + A_{\text{cells}})} \quad (9)$$

$$\eta_{\text{module}} = \eta_{\text{cell}} \cdot (K_1 + K_2 - 1) \cdot \prod_{i=3}^m K_i \quad (10)$$

Eq. (9) and (10) gives the expression for cell efficiency and module efficiency. Where  $K_1$  and  $K_2$  are the loss factors related to the inactive module areas, mainly the border and cell spacing area.

Figure 2 shows the shingled cell overlap for ModuleCTM fabrication. Shingling of cell into 6 stripes are produced with 5 cuts.

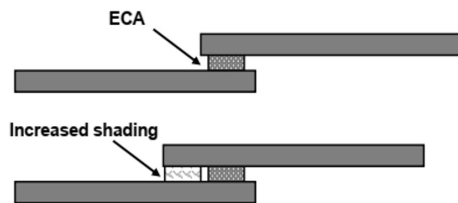


Fig. 2. Shingling cell overlap and reduce shading loss

### 3. CTM Loss Analysis

Shingled module is useful because here the cell overlap requires less silver usage in screen printing of cell grid resulting in the usage of less amount of ECA used for depositing interconnection. With cell overlap of about 0.8  $\text{mm}$  or less allows to save cells per module and consequently minimizes the material cost and CTM power loss. Other parameters such as alignment and total string strength are important to achieve uniform power output, reliability and aesthetic

consistency among all the strings. A shingled module can achieve  $P_{\text{mpp}}$  up to 340  $\text{W}$  using 83 shingled cells per string and 4 strings in parallel. FZ (Float zone) wafers can be used for many appliances such as in the manufacturing of power devices, solar cells and more as the contamination rate is very low compared to other wafer and process also purifies impurities which segregate in the melt. Because of high cost of FZ wafer, its applications are limited for special purpose only. Conventionally, CZ Si-Wafer, size 6", orientation: (100), boron doped, Resistivity: 0.001–100 ( $\text{ohm, Cm}$ ), 1 side polished having thickness 650  $\pm$  50  $\mu\text{m}$  is being used. This high thickness is incompatible for surface polishing on one side so 180  $\mu\text{m}$  wafer size is selected. Stripping of a cell can be done by a new process named LCD, without damaging the sliced edge of wafer. Since there is no dust formation so the cost of filtration unit can be eliminated completely. This reflects in the project cost reducing \$0.18 per cut for shingling cells. The technique is very much applicable for half-cut and shingled technology. An additional advantage of this technique is that the cell pieces produced by scribe and break method have lower mechanical strength compared to cleaved pieces. Also, it's feasible and least overlapping of cell area. Modern stripping technology is based on a wire sawing technique, where a thin wire (160  $\mu\text{m}$  diameter) web pushes an abrasive-based slurry into the silicon to be cut. The wire travelling speed can vary from 6–12  $\text{m/s}$ . The disadvantage with this technique is that it has poor cutting accuracy as the wire travels back and forth at high speed. The different process parameters for laser cutting technique namely (i) Power, (ii) Velocity, (ii) Spot diameter and (iv) Number of passes are taken into consideration.

Figure 3 is showing laser cutting of wafer allowed for precise lines to be cut since solar cells can be very fragile. It reduces the resistive losses and contributes

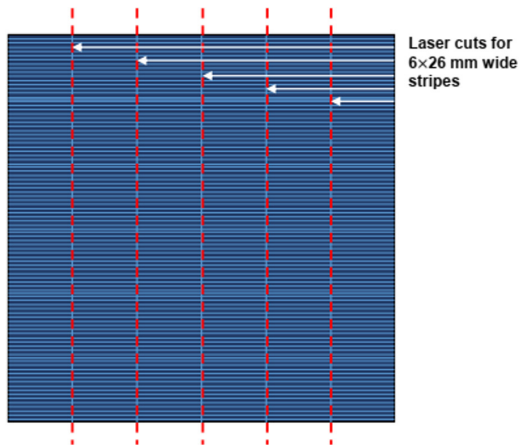


Fig. 3. Laser cutting of cell into 6 stripes

in increasing output power. First a groove is cut with a depth of about  $1/3^{\text{rd}}$  of wafer thickness and then mechanical force is applied to break the silicon slices exactly along the scribed line. Automation is required for mechanical separation of slices. Slicing of 6 stripes require 5 cuts. Now  $\text{CO}_2$  pulsed laser and plasma laser are commonly used for this purpose. There are other techniques available in the process industry for wafer cutting like thermal cutting, multi-pass cutting, gas assisted cutting, water jet cut, plasma cut and wire cut. Thermal cutting oriented fusion cutting shows smooth, flat and clean surface. The methodology mainly follows scribing & cleave and the wafer separation, produced by a snapping, either manually or automated. With the increase in speed, the visual aspect is more homogeneous through the cutting area. For speed value of 150 mm/s, it shows discontinuity despite of visual aspect are acceptable at first sight. A tight window of 150 to 170 mm/s can produce consistently smooth edge totally the brittle crack propagation<sup>[22]</sup>. Laser cutting is fast compared to others and can be used for mass production.

### 3.1 Methodologies to analyze the efficiency using different technologies

Every manufacturing industry is aiming to bring out

solutions for the technology which can give maximum module efficiency at a lower cost. Previously, studies were done on several factors that affect  $P_{mpp}$  and module area. The use of PERC cell technology can reduce the cell production to \$0.06. Compared to multi crystalline ( $\eta \sim 20\text{--}21\%$ ) PERC cells, mono-crystalline PERC cells are having an efficiency slightly higher of 21–22% around 2015 midway. Though technology progressed more and more in last few years. This research paper shows the recent progress in this aspect and it shows the future possibilities of further progress<sup>[23–27]</sup>. The performance of commercial PERC cells is much better compared to others in respect of  $V_{oc}$  as determined by cell  $J_0$  and resistive losses<sup>[28]</sup>. The estimated additional manufacturing cost of PERC cell including the wafer cost leveraged by higher efficiency is around 6%/W and at the module level the leveraging cost reduced to 2%/W. The factors on which the research work focus is to implement the PERC technology, to make highly efficient, increase and cost effective shingled cell.

However, this fabrication technique has some practical limit and further gain in efficiency is limited. The search for maximum efficiency has led the industry to adopt PERC technology. The Shingling approach can be applied to any cell architecture as long inter-connections are on the side of the cell. Using BSF, PERC, bifacial-PERC, n-PERT/PERL, HJ and others. The shingling technology shows different advantages in comparison to other PV modules i.e lower ohm losses, better area utilization, lower temperature processing, lower operating temperature and being made better aesthetics. In the shingled module, there is no cell gap so denser packing can be obtained. Because of small area utilization for shingled connected in series, it minimizes the ohm losses. When the cells are cut into strips, the photo generated current ( $I_{ph, cell}$ ) and the series resistance ( $R_s$ ) is affected,

The other parameters like diode saturation current ( $I_{oc}$ ), shunt resistance ( $R_{sh}$ ) and ideality factor of the diode ( $i_{idc}$ ) are kept constant. ECA's curing temperature is less than ribbon soldering, so the cells experience less amount of stress and bowing. Low operating temperature is related to increase in energy generation. Most of the features of shingled technologies giving advanced benefits leads to increase in an efficiency of the module.

Properties of  $SiN_x$  as AR coating having thickness of 80 nm, processed by plasma enhanced chemical vapor deposition, acts as an anti-reflection coating and can be utilized as excellent surface passivation layer, good metallization mask, diffusion barrier, chemical resistance, high temperature stability, low cost and throughput and good overall rating. AR layer structure is created with an oxide layer that provides efficient absorption of light and the efficiency of the structure increased to 24.4%. The cell parameters such as short circuit current ( $I_{sc}$ ) and fill factor (FF) vary with screen printing processing conditions mainly the aspect ratio and alignment. It depends on parameters like (i) wire dimension, (ii) mesh count and (iii) emulsion. Therefore, it is important to modify the metallization process to improve the performance of the solar cell.

### 3.2 ECA Material for cell interconnection

Conventional PV solar module technology are based on H-pattern cells, ribbons and soldered interconnections. This configuration has some disadvantages: (i) high shading loss (ii) expensive metallization (iii) high resistivity loss (iv) incompatible with very thin wafers and (v) load containing solder.

From Figure 4 it can be examined that for each cell stripe width it has an optimized amount of metallization finger metal line varies with respect to the maximum power of a shingled cell. From the simulated

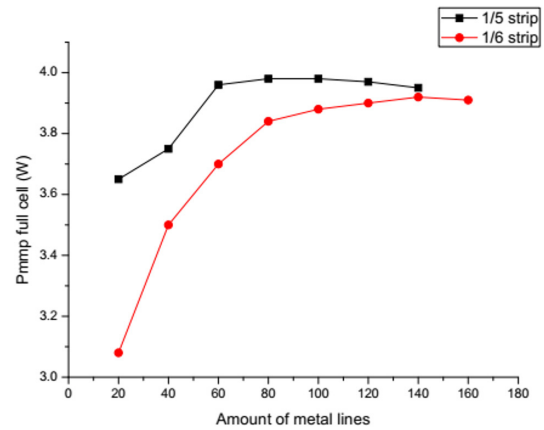


Fig. 4.  $P_{mpp}$  of full cell for variation width of cell strip assuming no further losses due to interconnection<sup>[29]</sup>

result it is concluded that even a lower amount of metallization line on the front side is enough to reach the maximum power point. Adhesion between joint material and metallization material needs to have excellent interconnection for Shingled technology which can be classified as (i) solder and (ii) ECA. Different types of ECA can be further classified as (i) Epoxy based, (ii) Acrylate based and (iii) Silicone based. Power degradation of the module is related to the loss in FF and  $I_{sc}$  based on increase in series resistance of module. This review article showed the most improved alternative of the interconnection material to reduce the CTM loss<sup>[30]</sup>. Table 1 shows the some solutions optimized for using in interconnection.

Graphene material has significant ( $\alpha=2,3\%$ ) fraction of incident white light having properties like zero bandgap semiconductor with a small overlap between

Table 1. Optimization of material solutions

	Eutectic tin lead solder	Epoxy ECA	Silicone ECA
G (MPa)	12000	200–2000	10–100
$\tau_{sh.str}$ (MPa)	40	5–10	0,3–1
$G / \tau_{sh.str}$	300	20–400	10–300
Resistivity (ohm cm)	$0,15 \times 10^{-4}$	$1-25 \times 10^{-4}$	$2-30 \times 10^{-4}$

valance and conduction band, excellent electrical conductivity and posing to a major challenge for graphene electronics. The graphene material has a fermi level of 0.16eV and dielectric grating with periodicity ( $d=130$  nm). The resistance of the ECA material is compared with silver and aluminum paste showing a low resistance value for ECA with silver paste.

Figure 5 explains the change in resistance with the change in length for two different pastes. Eutectic gallium–Indium binary alloy (EGaIn) is a combination of organic and inorganic material having non-toxicity, deformability, superior electrical properties, flexible and reconfigurable. The use of this material in the interconnection of shingled technology is quite advantageous as it is highly efficient with stretchable interconnections. The mechanical strength is 22% and electrical conductivity ( $\alpha=24,100$  S/cm). EGaIn shows advance properties over molted solders (used in the set of methodologies called micro solids) which need heating and cooling steps for the fabrication process and incompatible with heat-sensitive materials such as organics. Laser scanning microscope is used to show different ECA images. Electrical losses in shingled module depend on factors like (i) Cell

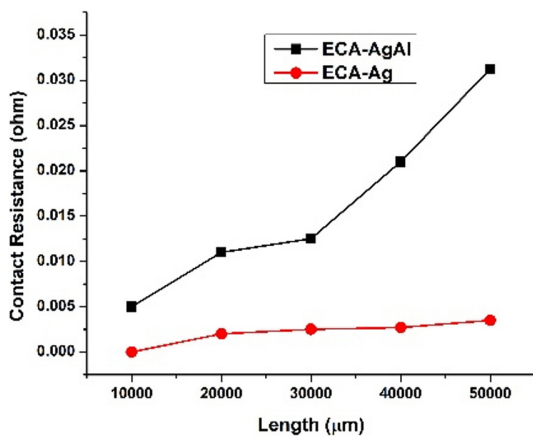


Fig. 5. Change in resistance with the change in length for ECA–AgAl and ECA–Ag paste

Interconnection and (ii) String Interconnection. The paste is applied to pneumatic dispenser on the MWT. The ECA paste is laminated using liquid silicone followed by curing which is done using liquid silicone at the standard process condition.

It can be seen, the results based on the EGaIn based interconnections maintain high electrical conductivity under severe elongation up to 95%, while silver pastes loose conductivity at an elongation of 0.6% and 60%, respectively. The contact resistance of EGaIn almost remains unchanged at a bending radius of  $\sim 1.5$  mm, at an angle of  $360^\circ$ , while in case of silver paste shows a large variation. The lifetime of a module can be increased by selecting proper interconnection material. Below Fig. 6 is showing a shingled module assembled with different layers.

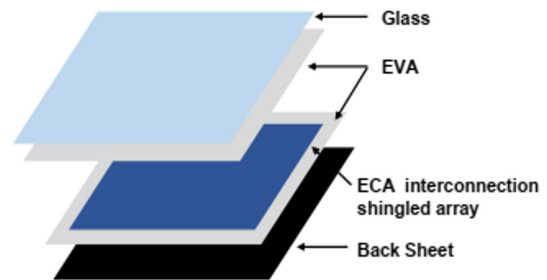


Fig. 6. Schematic diagram showing shingled module

### 3.3 EVA Material

The power loss due to encapsulant material is approximately 0.8 W which can be reduced by using excellent material such as EVA, back sheet and glasses are laminated by applying heat on both sends for protection. The module is finally completed with a frame. Different material combinations are used for module design such as Polyolefin (POE), Polyvinyl fluoride (TPT) and Ethylene Vinyl Acetate (EVA).

The elasticity of EVA and toughness of TPT together have wonderful property and protections. Now a days, conventional solar cells generally use TPT as

back-sheet substrate material, TPT as back-sheet material showed excellent durability, impermeability, insolubility, erosion durability, mechanical stability, and hydrophobic property. Thickness of the material is 0.32 mm and the breakdown voltage is approximately 17 KV. This encapsulant material can be fabricated between the double glass layer of thickness 22 mm for better absorption and prevention from mechanical stress.

### 3.4 Shingled Module design

To complete the study of shingled cell to module loss analysis, different module with 5 and 6 cell strips are optimized and found that with 6 strips the area utilization is improved. The two main area on which it is focused are the module area and maximum power point of a module. For design purpose, selection of wafer, cutting into strips, aligning them to form shingled cell to module, anti-reflection coating, shingled interconnection and module encapsulation are the key factors required. There are other factors like solar cell area, exposed module area, packing factor, electrical power output, module weight, encapsulation thickness, back sheet having white TPT, and thickness of interconnection contributes to the module design. Module dimension can be set according to the cell size, margins and overlap between shingled. The above-mentioned Si-wafer and 6 stripes per cell having inactive area of  $0.117 \text{ m}^2$  and overlap of 0.8 mm the dimension of shingled module can be designed as 6 stripes  $\times$  96 wafers in a module. The module can be designed using series parallel combination of cells i.e 12 cells in series and 8 cells in parallel. Conventional modules are having glass and back sheet as encapsulant material finally framing and substrate material. The above assemble the module size can be defined as  $1,8811,254 \text{ mm}^2$  having area

$2,358 \text{ m}^2$ , margin equal to 30 mm (top and bottom) 20 mm (left and right). As the interconnection loss optimization depends on the cell arrangement so the architecture of module is important. Also, with 96 cells, the module size will increase accommodating more shingled cells in the same area. The loss mechanism from cell to module depends on several factors as explained below. Cell spacing, (ii) Front to back cell Interconnection, (iii) Encapsulant cover, (iv) Module margin, (v) Interconnection coupling, (vi) String Interconnection, (vii) Electrical mismatch, (viii) Interconnection shading loss and (ix) Junction box and cabling. For module optimization these key factors play critical role in CTM loss.

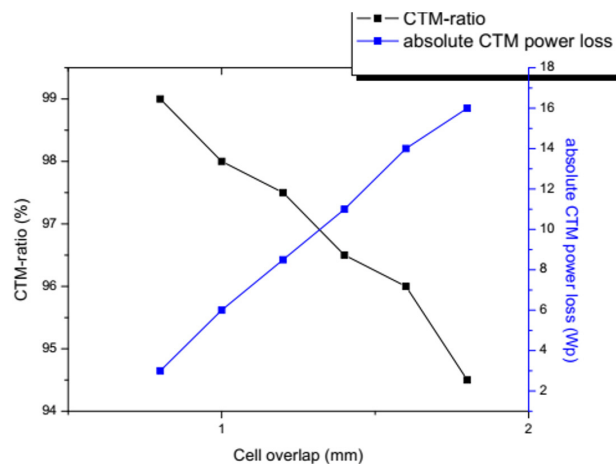


Fig. 7. Results showing overlap depth on CTM-power loss & CTM-ratio in Shingled modules

Shingled module uses no tabs between the cells (only between the strings). The series connection can be realized by stacking one edge over another like a roof shingled. These losses are calculated in percentage from the raw data after testing of module power and efficiency. Applying different material and technique some losses have been optimized in this paper and a proper conclusion has been drawn.

## 4. Conclusion and Future Scope

This review paper thoroughly investigated the advancement and future prospect of the Shingled module with c-Si solar cell. After a detailed study of different technologies, concluded that PERC technology with some better techniques can be used for optimizing maximum efficiency of Shingled cell to module with 6 strips. Shingled module have the potential to give an increase in power output by 10.3% compared to conventional module and it can increase the module efficiency approximately 1.83%. Different performance parameters are discussed along with the cell spacing, cell overlap, interconnection, encapsulant and lamination to increase the module efficiency. It is found that it can reach approximately 400 Wp output power and the CTM power ratio of 97.7% with PERC cell efficiency of 24.4%. There are several other internal parameters like module margin, cell spacing cover reflection and absorption, interconnection shading, finger coupling, cover coupling, electrical mismatch, junction box and cabling are very crucial in increasing the module efficiency. The CTM power loss can be reduced further to 1.24% by taking care of all these parameters. In this review paper, different materials for encapsulation and interconnection are studied and found that HIP MWT with EGaIn pastes for cell interconnection can further improve the module power output. FF nearly 80% is achievable with Ni/Cu based metal electrode contacts and 1.7% increase in cell efficiency using the methodology of LIP process with no observable degradation loss after a stress test. This technique not only into efficiency but also minimizes the production cost of the solar cells by approximately \$0.06. The future scope for this study is to further increase the module power output and cell efficiency by using bifacial PERC+ technology for space and other applications. It has been closely examined that PERC+

technology with minimum degradation losses can be used for the design implementation of Shingled cell to module. Shingled module can be applied using different interconnection materials.

## Acknowledgments

This work was supported by the Korea Institute of Energy Technology Evaluation and Planning (KETEP) and the Ministry of Trade, Industry and Energy (MOTIE) of the Republic of Korea (No. 20193010014850 & 202030301060).

## References

- [1] Scientific American, 2013, “Sun-roof: solar panel shingles come down in price, gain in popularity”, <https://www.scientificamerican.com/article/im-getting-my-roof-redone-and-heard-about-solar-shingles/>
- [2] White, W., 2017, “Real Goods Solar, Inc. (RGSE) stock skyrockets on dow deal”, <https://finance.yahoo.com/news/real-goods-solar-inc-rgse-155428529.html>
- [3] Summhammer, J., and Halavani, Z., 2013, “High-voltage PV modules with crystalline silicon solar cells”, Proceedings of the 28th European Photovoltaic Solar Energy Conference and Exhibition (28th EU PVSEC), 3119-3122.
- [4] Beaucarne, G., 2016, “Materials challenge for shingled cells interconnection”, Energy Procedia, **98**, 115-124.
- [5] Woehrl, N., Lohmüller, E., Mittag, M., Moldovan, A., Baliozian, P., Fellmeth, T., Krauss, K., Kraft, A., and Preu, R., 2017, “Solar cell demand for bifacial and singulated-cell module architectures”, 36th Photovoltaic International, 48-62.
- [6] Baliozian, P., Lohmüller, E., Fellmeth, T., Wöhrle, N., Krieg, A., and Preu, R., 2018 “Bifacial shingle solar cells on p-type Cz-Si (pSPEER)”, AIP Conference Proceedings, **1999**, 11002.
- [7] Rabanal-Arabach, J., Rudolph, D., Ullmann, I., Halm,

- A., Schneider, A., and Fischer, T., 2017, "Cell-to-module conversion loss simulation for shingled-cell concept", Proceedings of the 33rd European Photovoltaic Solar Energy Conference and Exhibition (EU PVSEC), 178-182.
- [8] Sung, E., and Zu-Li Liu, J., 2017, "Systems, method and apparatus for curing", U.S. Patent No. 9,748,434B1 (issued 29 August, 2017).
- [9] Morad, R., Almogy, G., Suez, I., Hummel, J., Beckett, N., and Lin, Y., 2016, "Shingled solar cell module", U.S. Patent No. 9,484,484B2 (issued 1 November 2016).
- [10] Radouane, K., Lutun, E., Binesti, D., Dupeyrat, P., Chiodetti, M., and Lindsay, A., 2015, "Key elements in the design of bifacial PV power plants", Proceedings of the 31st European Photovoltaic Solar Energy Conference and Exhibition, 1764-1769.
- [11] Kreinin, L., Bordin, N., Karsenty, A., Drori, A., and Eisenberg, N., 2011, "Experimental analysis of the increases in energy generation of bifacial over monofacial PV modules" Proceedings of the 26th European Photovoltaics Solar Energy Conference and Exhibition, 3140-3143.
- [12] Mittag, M., Zech, T., Wiese, M., Blasi, D., Ebert, M., and Wirth, H., 2017, "Cell-to-Module (CTM) analysis for photovoltaic modules with shingled solar cells", Proceedings of the IEEE 44th Photovoltaic Specialist Conference (PVSC), 1531-1536.
- [13] Guo, S., Singh, J.P., Peters, M., Aberle, A.G., and Wong, J., 2016, "Two-dimensional current flow in stringed PV cells and its influence on the cell-to-module resistive losses", *Solar Energy*, **130**, 224-231.
- [14] Kasahara, N., Yoshioka, K. and Saitoh, T., 2003, "Performance evaluation of bifacial photovoltaic modules for urban application", Proceedings of the 3rd World Conference on Photovoltaic Energy Conversion, **3**, 2455-2458.
- [15] Singh, J.P., Chai, J., Saw, M.H., and Khoo, Y.S., 2017, "Bifacial solar cell measurements under standard test conditions and the impact on cell-to-module loss analysis", *Jpn. J. Appl. Phys.*, **56**(8S2), 08MD04.
- [16] Green, M.A., Emery, K., King, D.L., and Igari, S., 2000, "Solar cell efficiency tables (version 15)", *Prog. Photovolt: Res. Appl.*, **8**(1), 187-195.
- [17] Singh, J.P., Khoo, Y.S., Chai, J., Liu, Z., and Wang, Y., 2016, "Cell-to-module power loss/gain analysis of silicon wafer-based PV modules", *Photovoltaics International*, **31**, 98-105.
- [18] Dickson, J.D.C., 1960, "Photo-voltaic semiconductor apparatus or the like", Hoffman Electronics Corp., U.S. Patent No. 2,938,938A (issued 31 May, 1960).
- [19] Leinkram, C., Oaks, W., 1973, "Shingled array of solar cells", U.S. Secretary of Navy, U.S. Patent No. 3,769,091A (issued 30 October 1973).
- [20] Romero, P., Otero, N., Coto, I., Leira, C., and González, A., 2013, "Experimental study of diode laser cutting of silicon by means of water assisted thermally driven separation mechanism", *Phys. Procedia*, **41**, 617-626.
- [21] Shi, Z., Wenham, S., and Ji, J., 2009, "Mass production of the innovative PLUTO solar cell technology", Proceedings of the 34th IEEE Photovoltaic Specialists Conference (PVSC), 001922-001926.
- [22] Wang, Z., Han, P., Lu, H., Qian, H., Chen, L., Meng, Q., Tang, N., Gao, F., Jiang, Y., Wu, J., et al., 2012, "Advanced PERC and PERL production cells with 20.3% record efficiency for standard commercial p-type silicon wafers", *Prog. Photovolt: Res. Appl.*, **20**(3), 260-268.
- [23] Müller, M., Altermatt, P.P., Wagner, H., and Fischer, G., 2013, "Sensitivity analysis of industrial multicrystalline PERC silicon solar cells by means of 3-D device simulation and metamodelling", *IEEE J. Photovolt.*, **4**(1), 107-113.
- [24] Altermatt, P.P., and McIntosh, K.R., 2014, "A roadmap for PERC cell efficiency towards 22%, focused on technology-related constraints", *Energy Procedia*, **55**, 17-21.
- [25] Fischer, G., Strauch, K., Weber, T., Müller, M., Wolny, F., Schiepe, R., Fülle, A., Lottspeich, F., Steckemetz, S., Schneiderloechner, E., et al., 2014, "Simulation based development of industrial PERC cell production beyond 20.5% efficiency", *Energy Procedia*, **55**, 425-430.
- [26] Min, B., Wagner-Mohnsen, H., Müller, M., Neuhaus, H., Brendel, R. and Altermatt, P.P., 2015, "Incremental efficiency improvements of mass-produced PERC cells

- up to 24%, predicted solely with continuous development of existing technologies and wafer materials”, Proceedings of the 31st European Photovoltaic Solar Energy Conference and Exhibition, 473-476.
- [27] Rudolph, D., Rabanal-Arabach, J., Ullmann, I., Halm, A., Schneider, A., and Fischer, T., 2003, “Cell design optimization for shingled modules”, Proceedings of the 33rd EU-PVSEC, 880-883.
- [28] Klasen, N., Mondon, A., Kraft, A., and Eitner, U., 2017, “Shingled cell interconnection: A new generation of bifacial PV-modules”, Proceedings of the 7th Workshop on Metallization and Interconnection for Crystalline Silicon Solar Cells.
- [29] Zhao, J., Wang, A., Abbaspour-Sani, E., Yun, F., and Green, M.A., 1997, “Improved efficiency silicon solar cell module”, IEEE Electron Device Letters, **18**(2), 48-50
- [30] Izzi, M., Tucci, M., Veneri, P.D., Scalari, S., Proietti, D., Colletti, C., Balucani, M., and Serenelli, L., 2018, “AMPERE: An european project aimed to decrease the levelized cost of energy with innovative heterojunction bifacial module solution ready for the market”, Proceedings of the 2018 IEEE 7th World Conference on Photovoltaic Energy Conversion (WCPEC), 569-572.